Variation of M×××H–C interactions in square-planar complexes of nickel(II), palladium(II), and platinum(II) probed by luminescence spectroscopy and X-ray diffraction at variable pressure

Stéphanie Poirier, Hudson Lynn, Christian Reber, Élodie Tailleur, Mathieu Marchivie, Philippe Guionneau, Michael Probert

Variation of M···H-C interactions in square-planar complexes of nickel(II), palladium(II), and platinum(II) probed by luminescence spectroscopy and X-ray diffraction at variable pressure

Stéphanie Poirier,[a] Hudson Lynn,[a] Christian Reber [*a]

[a] Département de Chimie, Université de Montréal, Montréal, Québec H3C 3J7, Canada

Elodie Tailleur,[b] Mathieu Marchivie,[b] Philippe Guionneau,[b]

[b] CNRS, Univ. Bordeaux, ICMCB, UMR 5026, 87 avenue du Dr A. Schweitzer, F-33608 Pessac, France

Michael R. Probert[c]

[c] Chemistry, School of Natural and Environmental Sciences, Newcastle University, Newcastle upon Tyne, NE1 7RU, United Kingdom

Synopsis

A detailed comparison of the solid-state d-d luminescence spectra of isoelectronic bis(dimethyldithiocarbamato) complexes of nickel(II), palladium(II), and platinum(II) is presented, including their deuterated analogs. Variable-pressure spectroscopy, high-resolution X-ray diffraction and variable-pressure X-ray diffraction reveal clear differences in molecular electronic structures and intermolecular interactions involving metal centers and methyl groups.

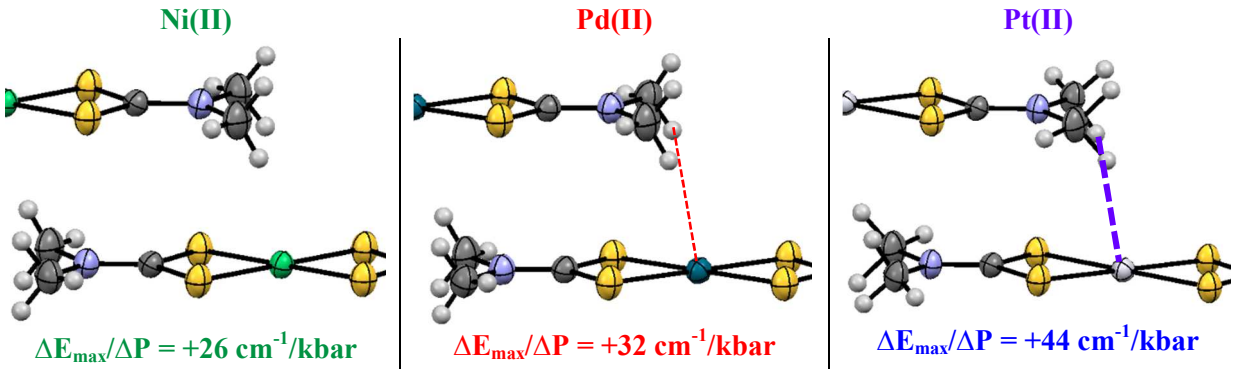

Abstract

Luminescence spectra of isoelectronic square-planar d^8 complexes with 3d, 4d and 5d metal centers show d-d luminescence with an energetic order different from the spectrochemical series, indicating that additional structural effects, such as different ligand-metal-ligand angles are important factors. Variable-pressure luminescence spectra of square-planar nickel(II), palladium(II), and platinum(II) complexes with dimethyldithiocarbamate ($\{CH_3\}_2DTC$) ligands and their deuterated analogs show unexpected variations of the shifts of their maxima. High-resolution crystal structures and crystal structures at variable pressure for $[Pt\{(CH_3)_2DTC\}_2]$ indicate that intermolecular M···H-C interactions are at the origin of these different shifts.

Introduction

A renewed focus on luminescence and photochemical properties of 3d complexes is emerging in the recent literature.[1-4] Many past studies are aimed at intensely luminescent complexes of 4d and 5d metals with d^6, d^8 or d^{10} electron configurations, documented in several comprehensive reviews.[5-8] Very few studies compare systematically the luminescence proprieties of 3d, 4d and 5d metal complexes with identical ligands. Variable-pressure studies provide quantitative, continuously varied spectroscopic properties of crystalline complexes,[9-11] and are especially attractive to probe structure-energy relations.[12-15] Only rarely have such continuous variations been explored by any spectroscopic technique for isoelectronic complexes with different metal centers. In this report, we compare variable-pressure luminescence spectra of structurally similar d^8 complexes with identical ligands, but different metal centers to quantify luminescence energy variations. Square-planar nickel(II), palladium(II), and platinum(II) complexes show luminescence in a variety of crystalline environments, in some cases affected by interactions perpendicular to the ML_4 plane.[5, 7]

Pressure induces an energy increase of the d-d luminescence maxima (E_{max}) from both octahedral and square-planar complexes.[12, 16] This increase is formally equivalent in both structures and can be rationalized using metal-ligand bonding characteristics. Metal-ligand bond lengths are compressed, leading to a stronger destabilization of the σ* LUMO than the π* HOMO, increasing their energy difference. This energy variation is comparable in size for a number of complexes with many different metal centers.[17] For square-planar complexes of palladium(II) and platinum(II) with chelating dithiocarbamate ligands, the average shift $\Delta E_{max}/\Delta P$ caused by bond compression is on the order of +12 ± 2 cm^{-1}/kbar.[17] It is expected that isoelectronic square-planar nickel(II) complexes also show shifts of this magnitude.[17] Deviations from this average value point towards additional effects. Illustrative examples

are the negative $\Delta E_{max}/\Delta P$ values for complexes with intermolecular metal-metal interactions. Tetracyanoplatinate(II) complexes show $\Delta E_{max}/\Delta P$ values of -115 to -320 cm^{-1}/kbar.[18] Square-planar nickel(II), palladium(II), and platinum(II) complexes with glyoxime ligands also show metal-metal interactions, and negative $\Delta E_{max}/\Delta P$ values are determined from the absorption spectra at variable pressure.[19] In these examples, increasing pressure leads to shorter metal-metal distances and stronger intermolecular interactions, inducing a gradual destabilization of the HOMO. The different isoelectronic metal centers involved in the metal-metal interaction greatly influence the variation of the absorption maxima for the glyoxime complexes.[19, 20] The nickel(II) complexes presented in the following show $\Delta E_{max}/\Delta P$ values closest to the literature range of +8 to +20 cm^{-1}/kbar for octahedral nickel(II) complexes from absorption data.[17] The $\Delta E_{max}/\Delta P$ values are significantly higher for the palladium(II) and platinum(II) analogs.[17]

Examples of intermolecular M···H-C interactions have been reported for square-planar platinum(II) and palladium(II) complexes.[21 22] These interactions are the focus of reports from several areas,[23-25] including crystal engineering[26, 27] or C-H activation.[28, 29] Experimental examples of such effects are often measured at a single set of conditions, which gives limited insight on the interaction and the effect of different metal centers.[24] These weak M···H-C interactions are challenging to describe theoretically[30] and experimental data is essential for any comparison, motivating our study covering 3d, 4d and 5d complexes.

The traditional ligand field picture for octahedral complexes with identical ligator atoms predicts an increasing energy splitting Δ_{oct} (between t_{2g} and e_g orbital energies) from 3d to 5d metal centers.[31] The expected energetic order for group 10 is nickel(II) << palladium(II) < platinum(II). The more extended 4d and 5d orbitals contribute to stronger metal-ligand bonding, leading to high Δ_{oct} values.[32] The difference between 4d and 5d complexes is smaller than between 3d and 4d, as illustrated with $[M(NH_3)_6]^{3+}$ complexes of group 9 metals, whose Δ_{oct} values vary from roughly 23000 cm^{-1} for cobalt(III), to 34000 cm^{-1} for rhodium(III) and 41000 cm^{-1} for iridium(III).[31, 33] This increase is approximately 50% from 3d to 4d, and 20% from 4d to 5d. Similar variations are also observed from the luminescence maxima E_{max} of $K_3[M(CN)_6]$ involving isoelectronic group 9 metal centers.[34] For square-planar complexes, the same trend is expected by formal analogy with octahedral complexes. The lowest energy d-d transition occurs between a $^3\Gamma$ excited state and the $^1\Gamma$ ground state. A difference of E_{max} by 15% is observed between palladium(II) and platinum(II) in square-planar halide complexes.[35, 36] The *bis*-diethyldithiocarbamate (EDTC) complexes of palladium(II) and platinum(II) show an increase of E_{max} by 11%.[37] The differences between square-planar palladium(II) and platinum(II) have been established,[38] and are similar to variations for octahedral 4d and 5d complexes. Data for nickel(II) analogs are essential to a systematic comparison of group 10 metal complexes. To the best of our knowledge, this is the first such comparison.

Solid-state luminescence spectra of square-planar nickel(II), palladium(II) and platinum(II) complexes with identical ligands are presented, all showing d-d transitions. We chose dimethyldithiocarbamate ligands ($\{CH_3\}_2$DTC), since their palladium(II) and platinum(II) complexes are reported to show unexpected shifts of the luminescence maxima with pressure.[17, 39] In the following, we complete the series with the nickel(II) complex and deuterated analogs of all metal centers. Variable pressure was used to induce gradual intramolecular and intermolecular structural variations, allowing us to characterize the effect of the interaction on the different metal centers. These spectroscopic results are combined with new structural data, in particular ambient pressure high-resolution crystal structures for all complexes to determine hydrogen and deuterium positions in order to correlate with the variation of the luminescence spectra. Crystal structures at variable pressure were determined for $[Pt\{(CH_3)_2DTC\}_2]$ to characterize the structural variations influencing intermolecular Pt···H-C interactions.

Results

Luminescence spectra

Luminescence spectra at ambient pressure and 80 K for the $[M\{(CH_3)_2DTC\}_2]$ complexes are presented in Figure 1. To the best of our knowledge, this is the first comparison of d-d luminescence measurements in the solid state for complexes of nickel(II), palladium(II), and platinum(II) with identical ligands. Luminescence maximum E_{max} is 14200 cm^{-1} for the nickel(II) complex, surprisingly higher in energy than for palladium(II) and platinum(II), with E_{max} values of 13300 cm^{-1} and 13800 cm^{-1}, respectively.

Variable-temperature spectra of $[Pd\{(CH_3)_2DTC\}_2]$ and $[Pt\{(CH_3)_2DTC\}_2]$[40] are compared to $[Ni\{(CH_3)_2DTC\}_2]$ spectra in Figure S1 (Supporting Information), the latter showing a shift of the luminescence maxima to lower energy as temperature increases. $[Ni\{(CH_3)_2DTC\}_2]$ spectra show constant bandwidth and shift more clearly than those of corresponding palladium(II) or platinum(II) complexes. Spectra are also presented for the deuterated analogs, with $\Delta E_{max}/\Delta T$ shifts shown in Figure S2 and Table S1. The nickel(II) complexes show the smallest difference between the spectra of non-deuterated and deuterated analogs with similar shapes and similar $\Delta E_{max}/\Delta T$ shifts. For both palladium(II) and platinum(II) the absolute values of the $\Delta E_{max}/\Delta T$ shifts are higher for the deuterated complexes than for the non-deuterated analogs. The bandshape of the deuterated platinum(II) complex at ambient conditions is much broader than for the non-deuterated analog.

Luminescence spectra at variable pressure are published for $[Pd\{(CH_3)_2DTC\}_2]$[17] and $[Pd\{(CD_3)_2DTC\}_2]$[17] and are presented for all complexes in Figure 2. For $[Pt\{(CH_3)_2DTC\}_2]$,[39] data at

pressures higher than 40 kbar are added here. For all complexes, a shift of E_{max} to higher energy from ambient pressure to roughly 20 kbar is observed, as shown in Figure 3. The values of $\Delta E_{max}/\Delta P$ are +26 ± 5 cm^{-1}/kbar, +32 ± 3 cm^{-1}/kbar and +44 ± 5 cm^{-1}/kbar for [Ni{$(CH_3)_2$DTC}$_2$], [Pd{$(CH_3)_2$DTC}$_2$] and [Pt{$(CH_3)_2$DTC}$_2$] complexes, respectively, as given in Table 1. At higher pressure, the $\Delta E_{max}/\Delta P$ values change for each complex. [Ni{$(CH_3)_2$DTC}$_2$] shows a negative $\Delta E_{max}/\Delta P$ value at pressures higher than 24 kbar. A negative shift is also observed for [Pt{$(CH_3)_2$DTC}$_2$] at pressures higher than 35 kbar. The [Pd{$(CH_3)_2$DTC}$_2$] complex is the only one showing three different $\Delta E_{max}/\Delta P$ values, with a value of +11 ± 3 cm^{-1}/kbar from 21 kbar to 45 kbar and a negative shift at pressures higher than 45 kbar.

The deuterated nickel(II) complex shows a $\Delta E_{max}/\Delta P$ value of +20 ± 5 cm^{-1}/kbar, similar to [Ni{$(CH_3)_2$DTC}$_2$] above. In contrast, significant differences between the non-deuterated and deuterated complexes occur for the palladium(II) and platinum(II) metal centers. For [Pd{$(CD_3)_2$DTC}$_2$], the $\Delta E_{max}/\Delta P$ value is higher by a factor of two than for the non-deuterated analog in the 0-20 kbar pressure range, with a value of +63 ± 8 cm^{-1}/kbar. The shifts become identical in the 20-45 kbar range, with a value of +12 ± 5 cm^{-1}/kbar. For [Pt{$(CD_3)_2$DTC}$_2$], spectra show significantly broader bands at low pressure, as seen in Figure 2f. This is indicative of two overlapping emission bands.

Raman spectra

Raman spectra at variable-pressure of [Pd{$(CH_3)_2$DTC}$_2$][17] and [Pd{$(CD_3)_2$DTC}$_2$][17] are published. Comparison of the spectra of non-deuterated and deuterated nickel(II), palladium(II), and platinum(II) complexes are shown in Figures S3 and S4, respectively. Raman spectra at variable temperature are shown in Figures S5 and S6. Each spectrum keeps a constant peak pattern, with no appearance or disappearance of peaks. Broadening can be seen at high pressure, attributed to crystal defects induced by pressure as previously reported.[41] Raman peak maxima at variable pressure are plotted in Figures S7, S8 and S9 for the [M{$(CH_3)_2$DTC}$_2$] complexes. They show gradual increases of vibrational frequencies with pressure due to bond length compression.[42] To correlate the effect of the intermolecular M···H-C interaction, C-H peaks are followed and are expected to change in accordance with the observations in the luminescence spectra. The [Pd{$(CH_3)_2$DTC}$_2$] complex shows a variation of the slope with pressure for its 2920 cm^{-1} vibration, from +0.45 ± 0.03 cm^{-1}/kbar to 0.0 ± 0.1 cm^{-1}/kbar, corresponding to a C-H mode. Surprisingly, no variations are observed in the platinum(II) and nickel(II) analogs, nor in any of the deuterated complexes. Calculated Raman spectra show a good agreement with the experimental spectra, as presented in Figures S10 and S11.

Ambient condition crystal structures

In most crystal structures of molecular materials, the positions of hydrogen or deuterium atoms are determined on the basis of theoretical (steric) considerations and are neither experimentally derived from electronic density maps nor refined. Since this is problematic for detailed distances and angles of M···H-C intermolecular contacts, single-crystal X-ray diffraction studies have been performed on the six compounds. The aim of these new high-resolution diffraction experiments was to precisely locate experimentally the positions of hydrogen (deuterium) atoms,[43] which is possible using diffractometers.[44] To be successful, this approach must be performed on highly diffracting samples, showing Bragg peaks far beyond the standard resolution of 0.77 Å, the value used in previous studies. We take advantage of the high quality of diffraction of the six compounds, whose Bragg peaks were collected up to 0.55 Å for all compounds. The high-resolution data collection significantly increases the number of observed reflections, allowing to safely add the hydrogen atom positions to the refinement. High-resolution crystal structures were therefore determined mostly in order to obtain experimental hydrogen or deuterium positions and precise M···H intermolecular distances and angles, as presented in Figure 4 and S12.

It is interesting to note that the calculated positions for H and D in the previously reported structures[17, 40] are close to the experimental positions obtained here, as shown in Table S2. *A posteriori*, it is possible to validate the model previously used to calculate the position of the hydrogen atoms in the present compounds. This result is of importance since intermolecular distances involving hydrogen atoms are very often discussed, but rarely experimentally determined in this kind of compounds. By extension, this validation may be applied to all previous study of luminescent complexes of the same family as well as the high-pressure data below.

Table 2 shows selected bond lengths and angles for [Ni{$(CH_3)_2$DTC}$_2$], [Pd{$(CH_3)_2$DTC}$_2$] and [Pt{$(CH_3)_2$DTC}$_2$] and their deuterated analogs. The palladium(II) and platinum(II) complexes are isostructural. The nickel(II) complex is slightly different, with shorter metal-ligand bond lengths and larger S-M-S angles. This is coherent with the smaller ionic radius of 0.49 Å for nickel(II) compared to palladium(II) and platinum(II), with values of 0.64 Å and 0.60 Å, respectively.[45] The difference between both M-S bonds lengths for [Ni{$(CH_3)_2$DTC}$_2$] and [Pd{$(CH_3)_2$DTC}$_2$] is 0.12 Å, close to their difference of ionic radii of 0.15 Å. In contrast, the differences of M-S bond lengths in [Pd{$(CH_3)_2$DTC}$_2$] and [Pt{$(CH_3)_2$DTC}$_2$] are only 0.005 Å and 0.001 Å. The same trends are observed for the deuterated complexes. Table 3 shows selected intermolecular distances and angles notably involving hydrogen (deuterium) atoms for [Ni{$(CH_3)_2$DTC}$_2$], [Pd{$(CH_3)_2$DTC}$_2$] and [Pt{$(CH_3)_2$DTC}$_2$] and their deuterated analogs. Deuteration has almost no effect on the geometry of the related intermolecular contacts, differences between M···H and M···D distances are within experimental precision. The geometry of M···H-C

(M···D-C) contacts is identical for palladium(II) and platinum(II) complexes. Globally, these contacts are also the same in the nickel(II) complex but a closer examination shows a significant shortening of the M···C distances compared to palladium(II) and platinum(II) analogs. Nickel(II) complexes show slightly shorter intermolecular M···H distances of 2.89(7) Å compared to 3.01(3) Å and 2.99(6) Å for palladium(II) and platinum(II), respectively. For the deuterated analogs, the M···D distances for the three complexes are identical within experimental precision, with values of 2.96(6) Å, 3.00(8) Å and 3.1(3) Å for nickel(II), palladium(II), and platinum(II), respectively. The analysis of the four S-M···H angles reveals a slightly better alignment of the M···H interaction in a direction perpendicular to the molecular plane for the nickel(II) complex, with angles closer to 90° than for the palladium(II) and platinum(II) complexes.

Variable pressure structure

The crystal structure determination of molecular materials under high-pressure by X-ray diffraction is more and more achievable yet still pioneering[46] especially when looking for accurate atomic positions.[47] The crystal structure at variable pressure has been determined for $[Pt\{(CH_3)_2DTC\}_2]$ in order to compare structural changes and variation of the luminescence spectra with pressure. We chose the platinum(II) complex as it shows the greatest shift of the luminescence maxima in the ambient pressure to 20 kbar range. Crystal structures were determined at 5 kbar and 10 kbar for the $[Pt\{(CH_3)_2DTC\}_2]$ complex using diamond-anvil cells (DAC). The crystallographic data is presented in Table S3, and shows a decrease of the unit-cell parameters and volume as pressure increases. From ambient pressure to 10 kbar, the unit-cell volume decreases by about 8% when a, b and c parameters decrease by 3%, 1.5% and 3.8% respectively. These values are significant and reveal a slight anisotropy of the high-pressure effects on the crystal packing. The pressure on the sample was increased up to 20 kbar but the diffraction pattern quality was too low to determine the crystal structures beyond 10 kbar. As seen from the diffraction patterns presented in Figure S13, broadening of the reflections increases gradually over the studied pressure range, indicating an alteration of the single-crystal quality at higher pressure in the pressure cell. This decrease of crystallinity is not a reversible phenomenon in this case and likely due to a degradation of the sample in this pressure range.

Selected bond lengths, angles, intermolecular distances and intermolecular angles are presented in Table 4. Compression of the metal-ligand bond lengths is too small to be determined in the measured pressure range. The C-N bond lengths vary with pressure and seem to slightly increase. The C-N-C angle between the methyl substituents is slightly compressed at higher pressure. Intermolecular distances are all reduced,

leading to a denser crystal packing at higher pressure, as shown in Figure S14. Interestingly, the intermolecular distances between the carbon and the metal for both methyl groups decrease anisotropically, with decreasing values from ambient pressure to 10 kbar of 3.89(6) Å, 3.84(4) Å and 3.82(9) Å for Pt···C(4) and of 4.39(4) Å, 4.34(4) Å and 4.18(6) Å for Pt···C(5), corresponding to a decrease of approximately 2% and 5% for Pt···C(4) and Pt···C(5), respectively. Rotation of the methyl with H(D) is observed as pressure is varied, but not for the methyl involved in the M···H-C interaction, as seen in Figure S15.

Discussion

Molecular structure and luminescence energy

At low temperature, the luminescence maximum E_{max} of the nickel(II) complex is higher in energy than for the palladium(II) and platinum(II) analogs. Even at ambient temperature, the E_{max} value of the nickel(II) complex stays higher in energy than for the palladium(II) complex. Ligand-field theory for perfectly square-planar coordination geometries predicts a lower energy for nickel(II), but chelating angles must be included in this comparison. For $[Ni\{(CH_3)_2DTC\}_2]$, the S-Ni-S angle of 79° is higher than for $[Pd\{(CH_3)_2DTC\}_2]$ or $[Pt\{(CH_3)_2DTC\}_2]$ which show an angle of 75°. This leads to a better orbital overlap for the M-S bonds, and therefore energies of the d orbitals are affected. This is shown in Figure 5 and S16 by angular overlap model (AOM) calculations where the S-M-S angle is varied from 70° to 90°. The HOMO-LUMO energy difference increases as the angle increases towards 90°, a key factor contributing to the high E_{max} observed for the nickel(II) complex. This angular structural variation leads to the unexpected E_{max} order for this series of complexes.

Luminescence spectra at variable temperature show a shift of E_{max} to lower energies occurring with a nearly constant bandwidth for nickel(II) complexes as temperatures increase. The shape of the band changes from asymmetric to more symmetric, which points to a dominant influence from a small structural variation as temperature is varied, as previously reported and analyzed for platinum(II) dithiocarbamate complexes.[39] Lower temperature leads to a decrease of the unit cell volume, which is qualitatively equivalent to an increase of pressure, from this overall point of view. The structural effect induces an increase of E_{max} as temperature decreases, the LUMO being more destabilized than the HOMO. The trend is qualitatively consistent with the negative $\Delta E_{max}/\Delta T$ shift of nickel(II) complexes as temperature increases. This structural effect is not dominant in the spectra of palladium(II) and platinum(II) analogs, as their structure are different from the nickel(II) complexes. Palladium(II) and platinum(II) complexes show broadening of their spectra towards lower and higher energy, respectively.

Broadening to lower energy is due to distortion in the excited state. Broadening to higher energy is due to thermal population of higher energy vibrational levels. The observed shifts are the results of these competing trends.[40]

In view of their similar structure, variations of the luminescence spectra are expected to be similar for deuterated and non-deuterated complexes. This is the case for the nickel(II) compounds. Surprisingly, the deuterated palladium(II) complex shows a significantly lower-energy maximum at 12200 cm^{-1} than $[Pd\{(CH_3)_2DTC\}_2]$ with a maximum at 13000 cm^{-1} at room temperature.[40] This difference is likely due to different intermolecular interactions. M···H(D)-C interaction appear to be stronger at ambient temperature for $[Pd\{(CD_3)_2DTC\}_2]$ than for $[Pd\{(CH_3)_2DTC\}_2]$, leading to a lower E_{max} value.[17] As temperature is lowered, this interaction weakens for both systems, giving a different $\Delta E_{max}/\Delta T$ slope for the deuterated analog. For the deuterated platinum(II) complexes, an important increase of the intensity on the high-energy side is measured, leading to a significantly broader band at room temperature. $[Pt\{(CH_3)_2DTC\}_2]$ shows a corresponding broadening, which is typical for vibronic intensity gain as temperature increase.[39, 40] The spectrum of $[Pt\{(CD_3)_2DTC\}_2]$ at 293 K, in Figure S1f, has a bandwidth of 5000 cm^{-1}, larger by 1000 cm^{-1} than for the non-deuterated complex at this temperature. This important difference cannot be accounted for by vibronic intensity gain. It is therefore suspected that $[Pt\{(CD_3)_2DTC\}_2]$ exhibits two overlapping emission bands from thermally populated excited states.

Pressure effects on luminescence spectra

The luminescence maxima of the $[M\{(CH_3)_2DTC\}_2]$ complexes show higher positive $\Delta E_{max}/\Delta P$ values than the average +12 ± 2 cm^{-1}/kbar expected[17] for square-planar dithiocarbamate complexes. These differences indicate that a stabilization of the HOMO occurs as pressure increases. In other words, intermolecular interactions present at ambient pressure are weakening as pressure increases, which leads to high positive values[38] of $\Delta E_{max}/\Delta P$ shown in Table 1 (0 to 20 kbar). $[Ni\{(CH_3)_2DTC\}_2]$ shows the lowest $\Delta E_{max}/\Delta P$ value of +26 ± 5 cm^{-1}/kbar among the metal complexes studied here, suggesting that it has the weakest M···H-C intermolecular effect on luminescence. This is rationalized by the smaller ionic radius of nickel(II) compared to palladium(II) and platinum(II). Literature examples of similar values of $\Delta E_{max}/\Delta P$ as $[Ni\{(CH_3)_2DTC\}_2]$ are reported for palladium(II) or platinum(II) complexes with S-M-S angles of 90°, as illustrated by the value of +29 cm^{-1}/kbar for $(n\text{-}Bu_4N)_2[Pd(SCN)_4]$.[48] In these complexes with monodentate ligands, the shift of the luminescence maxima is due to bond compression only, with no extra intermolecular interaction contributing. The $\Delta E_{max}/\Delta P$ value for $[Ni\{(CH_3)_2DTC\}_2]$ is due to bond compression and possibly a very weak interaction. The deuterated nickel(II) analog shows a similar

$\Delta E_{max}/\Delta P$ shift of +20 ± 5 cm^{-1}/kbar. This is expected from the high-resolution structures, with equivalent measured positions of H and D.

For $[Pd\{(CH_3)_2DTC\}_2]$ and $[Pt\{(CH_3)_2DTC\}_2]$, $\Delta E_{max}/\Delta P$ values are +32 ± 3 cm^{-1}/kbar and +44 ± 5 cm^{-1}/kbar, respectively. The higher $\Delta E_{max}/\Delta P$ value for $[Pt\{(CH_3)_2DTC\}_2]$ indicates a stronger destabilization of HOMO at ambient pressure, thus a stronger intermolecular interaction for the 5d metal than for the 4d analog. Structural differences alone cannot explain the differences observed in the luminescence spectra at variable pressure.

The $\Delta E_{max}/\Delta P$ for the deuterated palladium(II) compound is higher by a factor of two than for the non-deuterated analog, with values of +63 ± 8 cm^{-1}/kbar and +32 ± 3 cm^{-1}/kbar, respectively. This indicates a stronger intermolecular interaction with the deuterium than with the hydrogen. The Raman spectra in Figures S3 and S4 show C-D stretching at 2100-2300 cm^{-1}, lower than C-H stretching at 2900-3000 cm^{-1}.

Luminescence spectra of the deuterated platinum(II) complex show two transitions, despite identical crystal structures to the non-deuterated analog. The comparison of calculated energy levels in Figure S17 and S18 shows that both deuterated and non-deuterated platinum(II) complexes have a molecular orbital centered on the ligand (LUMO+1) close in energy to the LUMO, different from the palladium(II) or the nickel(II) complexes. The higher-energy emission measured for the deuterated platinum(II) complex is possibly due to a metal-to-ligand charge transfer from LUMO+1. It gains intensity due to less efficient non-radiative relaxation in deuterated systems.[49-51] As pressure increases, non-radiative processes become more efficient, leading to the gradual intensity loss of the higher-energy transition, disappearing completely at pressures above 25 kbar.

Pronounced spectroscopic differences are observed between deuterated and non-deuterated complexes of palladium(II) and platinum(II), showing different $\Delta E_{max}/\Delta P$ values and emission patterns, respectively. This shows that the presence of C-D bonds significantly affects the luminescence spectra, allowing the deuteration effect to be probed by luminescence spectroscopy at variable pressure. In marked contrast, deuterated and non-deuterated nickel(II) complexes show identical variations of $\Delta E_{max}/\Delta P$ values within the experimental precision. Therefore, deuteration does not affect their shift of the luminescence maxima, in contrast to palladium(II) and platinum(II) complexes. In view of the identical shifts for deuterated and non-deuterated nickel(II) complexes and their positive $\Delta E_{max}/\Delta P$ values within the range reported for complexes without interaction, we conclude that Ni···H(D)-C interactions have a negligible effect on the luminescence spectra.

Crystal structure at variable pressure

For [Pt{$(CH_3)_2$DTC}$_2$], intermolecular distances decrease as expected with pressure, but metal-ligand bonds are not significantly compressed within the studied pressure range (0-10 kbar). Changes in the intermolecular region are however measurable. Figure 6 shows a view of three molecules in the crystal structure at ambient pressure and 10 kbar, to highlight the intermolecular movement. The top panel of Figure 6 shows a decrease in the vertical distances at 10 kbar compared to ambient pressure. The top and bottom molecules get closer to the middle molecule at 10 kbar, clearly showing the decrease of intermolecular distances. A horizontal sliding of the complexes also occurs as pressure increases. The vertical red line aligned on the platinum(II) center of the middle molecule shows that the top and bottom molecules get more centered at higher pressure. On the second panel, a decrease of the intermolecular distances in the vertical axis is also visible, the top and bottom molecules getting closer to the middle one. A sliding of the molecules along the horizontal axis is observed. The top and bottom molecules are pushed out at higher pressure, highlighted by the vertical red line passing through the sulfur atom (yellow) of the middle molecule. At lower pressure, it is well aligned with the nitrogen (blue) of the top molecule, but at 10 kbar, the nitrogen is pushed on the left. The same observation is made with the bottom molecule, the nitrogen atom being shifted to the right at 10 kbar. In the last panel, the changes illustrated are minor. Movements described in the two last panels result in a diagonal sliding of the molecules in the bottom panel point of view. However, a change in both N-C bonds also occurs, increasing from 1.46(6) Å at ambient pressure to 1.54(9) Å at 10 kbar for C(5)-N and from 1.41(5) Å to 1.56(7) Å for C(4)-N, which makes the diagonal sliding harder to see directly. The red circle highlights the movement of the C(4), part of the Pt···H-C interaction. At high pressure, the C(4) is getting further from the S atoms underneath it, being pushed along the diagonal. This also causes the carbon to be pushed away from the platinum(II) center.

All the observations from the three panels and data from Table 4 show an increase of the misalignment between the CH_3 substituents and the platinum d_{z^2} orbital as pressure increases, due to sliding of the molecules. This misalignment weakens the M···H-C interaction, which causes the high positive $\Delta E_{max}/\Delta P$ value of +44 ± 5 cm^{-1}/kbar. A suitable compound for comparison is [Pt(SCN)$_2${(μ-SCN)Mn(NCS)(bipy)$_2$}$_2$].[21] This square-planar platinum(II) complex with thiocyanate ligands also shows a Pt···H-C interaction in its crystal structure. The d-d luminescence maxima shift to lower energy with pressure, with a $\Delta E_{max}/\Delta P$ value of -99 cm^{-1}/kbar.[21] In contrast to [Pt{$(CH_3)_2$DTC}$_2$], the crystal structure of [Pt(SCN)$_2${(μ-SCN)Mn(NCS)(bipy)$_2$}$_2$] shows a very good alignment between the metal center and the interacting hydrogen. The crystal packing prevents sliding of the complexes, and so, application of pressure results in a reduction of the intermolecular distance between interacting atoms. Therefore,

pressure induces a strengthening of the Pt···H-C interaction, resulting in a pronounced negative $\Delta E_{max}/\Delta P$ shift, in marked contrast to the observations for $[Pt\{(CH_3)_2DTC\}_2]$.

The sliding movement of the molecules in $[Pt\{(CH_3)_2DTC\}_2]$ leads to a partial loss of crystallinity that may cause broadening of the reflections in the diffraction pattern at pressure above 10 kbar due to increase of the crystal defects, presented in Figure S13. XRD clearly shows this phenomenon, absent in the luminescence spectra but also observed in the Raman spectra.

By extrapolation from this evolution of the crystal packing to higher pressure, the sliding of the molecules eventually causes the M···H-C interaction to be lost. Therefore, at a certain point, it is expected that the evolution of the luminescence maxima changes. If a new interaction occurs due to the decreasing intermolecular distances, a negative $\Delta E_{max}/\Delta P$ value should be measured. In accordance with this expectation this is indeed observed for all non-deuterated complexes, and it all occurs at specific pressures. For $[Ni\{(CH_3)_2DTC\}_2]$, the variation of the slope appears at 24 kbar, changing from +26 ± 5 cm^{-1}/kbar to a negative $\Delta E_{max}/\Delta P$ value of -15 ± 6 cm^{-1}/kbar. Since the intermolecular distances decrease with pressure, at one point, another intermolecular interaction with the metal center may occur, as experimentally shown with the negative value of $\Delta E_{max}/\Delta P$. For $[Pd\{(CH_3)_2DTC\}_2]$, the initial interaction is lost at the same pressure, at 21 kbar, showing a $\Delta E_{max}/\Delta P$ value falling in the average range of +12 ± 2 cm^{-1}/kbar. This indicates that, in that pressure region, the metal center has no additional interaction, the luminescence being influenced by bond compression only. Interestingly, at 45 kbar, a negative $\Delta E_{max}/\Delta P$ value of -31 ± 8 cm^{-1}/kbar is observed, indicating a new intermolecular interaction. For $[Pt\{(CH_3)_2DTC\}_2]$, the initial M···H-C interaction is lost at higher pressure than for the two previous complexes, where its $\Delta E_{max}/\Delta P$ changes at 40 kbar. Even tough platinum(II) and palladium(II) complexes are isostructural, with very similar intermolecular distances, no range without interaction is measured for $[Pt\{(CH_3)_2DTC\}_2]$. Instead, the luminescence maxima shift to lower energies, with an $\Delta E_{max}/\Delta P$ value of -37 ± 8 cm^{-1}/kbar, indicating a new dominant intermolecular interaction. Assuming identical intermolecular movement for isostructural complexes, this indicates a greater extent of the electronic density in the z axis for platinum(II), allowing the M···H-C intermolecular interaction to be persistent at greater intermolecular distance. This effect was also observed in a recent study on isostructural complexes of lanthanides with chelating metalloligands of palladium(II) and platinum(II), clearly showing by EPR that 5d metal complexes have a wider radial extension than their 4d analogs.[52] In the $[M\{(CH_3)_2DTC\}_2]$ complexes, the extended electronic density of the 5d metal allows the initial M···H-C interaction to be present at higher pressure, showing stronger intermolecular interactions for same intermolecular distances than 4d metal.

The subtle structural variations, affecting the weak M···H-C interactions are not evident in the Raman spectra measured at variable pressure. In Figures S7 to S9, a zoom in the 2900-3000 cm^{-1} region is presented to look specifically for peaks corresponding to vibrations that could be involved in M···H-C interactions. No variation of the slope presented in Figures S7 to S9 is observed in the 0-40 kbar region for all complexes despite very clear effects observed in the luminescence spectra. Broadening of the diffraction peaks observed in the high-pressure diffraction patterns of $[Pt\{(CH_3)_2DTC\}_2]$ at 15-20 kbar due to loss of crystallinity does not lead to much broader peaks in the Raman spectra, as the prominent Raman peaks correspond to localized molecular modes. Only one peak for $[Pd\{(CH_3)_2DTC\}_2]$ complex shows a very subtle change in its peak shift around 50 kbar, with values varying from $+0.45 \pm 0.03$ cm^{-1}/kbar to 0.0 ± 0.1 cm^{-1}/kbar, which could correspond to an additional interaction occurring at shorter intermolecular distances. X-ray crystal structures at variable pressure clearly show these small structural changes leading to new M···H(D)-C interactions that are too weak to be detected by Raman spectroscopy but clearly affecting luminescence spectra at variable pressure.

Conclusion

We present a detailed comparison of the luminescence properties of a series of square-planar nickel(II), palladium(II), and platinum(II) complexes. The smaller ionic radius of nickel(II) induces a larger S-M-S angle and crystal-packing differences compared to the 4d and 5d analogs, leading to higher-energy luminescence maxima E_{max} than expected. The luminescence spectra of $[Ni\{(CH_3)_2DTC\}_2]$ at pressures below 20 kbar show the blue shift expected for d-d transitions. This contrasts with the palladium(II) and platinum(II) analogs that both show pressure-induced shifts of their band maxima indicative of intermolecular interactions. Deuteration of the complexes does not lead to different shifts in the nickel(II) complexes, consistent with very weak intermolecular Ni···H(D)-C interactions, while it leads to stronger interactions in the palladium(II) complexes and to a multi-state emission for the deuterated platinum(II) complex. X-ray crystallography at variable pressure on $[Pt\{(CH_3)_2DTC\}_2]$ reveals a sliding of the layers containing complexes, leading to weaker M···H-C interaction, again consistent with the shifts of luminescence spectra at variable pressure. We conclude that significant differences in intermolecular interaction strength lead to the different shifts, qualitatively comparable to different radial electronic density along the axis perpendicular to the MS_4 coordination plane. Luminescence spectroscopy at variable pressure is shown to be a very sensitive technique, well suited to observe the subtle structural variations at the focus of this study. Combined with accurate and *in situ* crystallographic data, it is possible to obtain a detailed characterization of isoelectronic complexes with different metal centers, taking into account even weak M···H-C intermolecular interactions. The approach developed here

provides quantitative insight for understanding the differences of the luminescence properties for 3d, 4d and 5d complexes in the solid state.

Experimental details

Luminescence and Raman spectroscopy at variable pressure

Variable-pressure Raman and luminescence spectra of [Ni{$(CH_3)_2$DTC}$_2$], [Pd{$(CH_3)_2$DTC}$_2$] and [Pt{$(CH_3)_2$DTC}$_2$] and their deuterated analogs, [Ni{$(CD_3)_2$DTC}$_2$], [Pd{$(CD_3)_2$DTC}$_2$] and [Pt{$(CD_3)_2$DTC}$_2$], were measured using a Renishaw InVia spectrometer coupled to an imaging microscope (Leica). The 488 nm excitation wavelength from an Argon-ion laser was used for all luminescence measurements and a diode laser (785 nm excitation wavelength) for Raman spectra. Calibration of the spectrometer was made with a tungsten lamp and luminescence intensities in spectra are corrected for system response. The crystals were inserted in a stainless-steel gasket along with ruby, used for pressure calibration. Nujol oil was added as pressure-transmitting medium. Pressure was applied trough a diamond-anvil cell (DAC, High-Pressure Diamond Optics).

High-resolution X-ray diffraction

Single crystals of [Ni{$(CH_3)_2$DTC}$_2$], [Pd{$(CH_3)_2$DTC}$_2$] and [Pt{$(CH_3)_2$DTC}$_2$] and their deuterated analogs, [Ni{$(CD_3)_2$DTC}$_2$], [Pd{$(CD_3)_2$DTC}$_2$] and [Pt{$(CD_3)_2$DTC}$_2$] were mounted onto a Bruker-Apex II CCD at 293 K. The full collection of data was measured at a resolution of 0.55 Å, see text for justification. Hydrogen (deuterium) atoms positions were determined on difference Fourier maps and refined freely. Structural solutions and least squares refinements were carried out using an Olex2[53] interface to the SHELX[54, 55] suite of programs. The crystallographic data is presented in Tables S4 and S5.

Variable pressure X-ray diffraction

High-pressure experiments on [Pt{$(CH_3)_2$DTC}$_2$] were performed using a modified Merrill-Bassett diamond anvil cell (DAC). The single crystal sample was loaded into a stainless-steel gasket with ruby in the DAC to calibrate the pressure by measuring its luminescence peak. Pressure was measured before and after data collection. Paraffin oil was used as a pressure medium. High pressure X-ray single-crystal diffraction data were collected at room temperature on a the XIPHOS II instrument at Newcastle University.[56] This instrument was custom built for high pressure single crystal X-ray diffraction studies

with an Incoatec Ag Iμs Kα (λ = 0.56086 Å) source. Data were collected, using 10 phi scans to maximise accessible coverage. Ambient pressure, 5 kbar, 10 kbar, 15 kbar and 20 kbar data were measured, as well as ambient pressure after the pressure release. Sample reflections were identified using the reciprocal lattice viewer within the Apex II program[57] for initial unit cell refinement. The program ECLIPSE[58] was used to generate mask files for data integration. Data integration and global cell refinement were performed with the program SAINT[59] and data were corrected for absorption with the program SADABS.[60] The minimum transmission factor for the high-pressure structures is due to partial shadowing from the DAC gasket. Structural solutions and least squares refinements were carried out using the Olex2[53] interface to the SHELX[54, 55] suite of programs. Suitable structures were obtained for three pressures: ambient, 5 kbar and 10 kbar.

Associated Content

Supporting information

The Supporting Information is available free of charge on the ACS Publications website at DOI: XXX. Luminescence spectra and E_{max} at variable-temperature for all complexes, Raman spectra and peaks values at variable temperature and variable pressure for all complexes, the perspective views of high-resolution structure of deuterated complexes, crystallographic data for structures at high-resolution for all complexes, images of diffraction patterns for structures at variable pressure of $[Pt\{(CH_3)_2DTC\}_2]$, crystal packing views of $[Pt\{(CH_3)_2DTC\}_2]$ at variable pressure, results of AOM calculations, calculated MO energy levels for all complexes and representation of LUMO+1 for $[Pt\{(CH_3)_2DTC\}_2]$.

Accession Codes

CCDC 1583142-1583144 contains the supplementary crystallographic data for this paper. These data can be obtained free of charge via www.ccdc.cam.ac.uk/data_request/cif, or by emailing data_request@ccdc.cam.ac.uk, or by contacting The Cambridge Crystallographic Data Centre, 12 Union Road, Cambridge CB2 1EZ, UK; fax: +44 1223 336033.

Author Information

Corresponding Author
*E-mail: christian.reber@umontreal.ca Tel: +1 514-343-7332. Fax: + 1 514-343-7586.

ORCID
Christian Reber: 0000-0001-9350-7262

Notes
The authors declare no competing financial interest.

Acknowledgements

We thank the Natural Sciences and Engineering Research Council (NSERC, Canada) and Fonds de recherche du Québec - Nature et technologies (FRQNT) for research grants and for graduate scholarships to S.P. A Mitacs Globalink – Campus France international research scholarship to S.P. is gratefully acknowledged. We acknowledge the Labex Amadeus of the University of Bordeaux (France) for travelling supports and the Ministère de l'Enseignement supérieur, de la Recherche et de l'Innovation for a graduate scholarship to E.T.

References

(1) Otto, S.; Grabolle, M.; Forster, C.; Kreitner, C.; Resch-Genger, U.; Heinze, K. $[Cr(ddpd)_2]^{3+}$: A Molecular, Water-Soluble, Highly NIR-Emissive Ruby Analogue. *Angew. Chem. Int. Ed. Engl.* **2015,** *54*, 11572-11576.

(2) Büldt, L. A.; Wenger, O. S. Chromium complexes for luminescence, solar cells, photoredox catalysis, upconversion, and phototriggered NO release. *Chem. Sci.* **2017,** *8*, 7359-7367.

(3) Otto, S.; Scholz, N.; Behnke, T.; Resch-Genger, U.; Heinze, K. Thermo-Chromium: A Contactless Optical Molecular Thermometer. *Chem. Eur. J.* **2017,** *23*, 12131-12135.

(4) Chabera, P.; Liu, Y.; Prakash, O.; Thyrhaug, E.; Nahhas, A. E.; Honarfar, A.; Essen, S.; Fredin, L. A.; Harlang, T. C.; Kjaer, K. S.; Handrup, K.; Ericson, F.; Tatsuno, H.; Morgan, K.; Schnadt, J.; Haggstrom, L.; Ericsson, T.; Sobkowiak, A.; Lidin, S.; Huang, P.; Styring, S.; Uhlig, J.; Bendix, J.; Lomoth, R.; Sundstrom, V.; Persson, P.; Warnmark, K. A low-spin Fe(III) complex with 100-ps ligand-to-metal charge transfer photoluminescence. *Nature* **2017,** *543*, 695-699.

(5) Yam, V. W. W.; Au, V. K.; Leung, S. Y. Light-Emitting Self-Assembled Materials Based on d^8 and d^{10} Transition Metal Complexes. *Chem. Rev.* **2015,** *115*, 7589-7728.

(6) Wenger, O. S. Vapochromism in organometallic and coordination complexes: chemical sensors for volatile organic compounds. *Chem. Rev.* **2013,** *113*, 3686-3733.

(7) Aliprandi, A.; Genovese, D.; Mauro, M.; De Cola, L. Recent Advances in Phosphorescent Pt(II) Complexes Featuring Metallophilic Interactions: Properties and Applications. *Chem. Lett.* **2015,** *44*, 1152-1169.

(8) Sun, Q.; Mosquera-Vazquez, S.; Suffren, Y.; Hankache, J.; Amstutz, N.; Lawson Daku, L. M.; Vauthey, E.; Hauser, A. On the role of ligand-field states for the photophysical properties of ruthenium(II) polypyridyl complexes. *Coord. Chem. Rev.* **2015,** *282-283*, 87-99.

(9) Byrne, P. J.; Richardson, P. J.; Chang, J.; Kusmartseva, A. F.; Allan, D. R.; Jones, A. C.; Kamenev, K. V.; Tasker, P. A.; Parsons, S. Piezochromism in nickel salicylaldoximato complexes: tuning crystal-field splitting with high pressure. *Chem. Eur. J.* **2012,** *18*, 7738-7748.

(10) Takagi, H. D.; Noda, K.; Itoh, S.; Iwatsuki, S. Piezochromism and Related Phenomena Exhibited by Palladium Complexes. *Plat. Met. Rev.* **2004,** *48*, 117-124.

(11) Reber, C.; Sonneville, C.; Poirier, S.; Bélanger-Desmarais, N.; Connick, W. B.; Chatterjee, S.; Franz, P.; Decurtins, S. In *RSC Specialist Periodical Reports: Spectroscopic Properties of Inorganic and Organometallic Compounds*; Yarwood, J., Douthwaite, R., Duckett, S. B., Ed.; The Royal Society of Chemistry: 2014; Vol. 45, pp 260-273.

(12) Parsons, R. W.; Drickamer, H. G. Effect of Pressure on the Spectra of Certain Transition Metal Complexes. *J. Chem. Phys.* **1958,** *29*, 930-937.

(13) Zahner, J. C.; Drickamer, H. G. Effect of Pressure on Crystal-Field Energy and Covalency in Octahedral Complexes of Ni^{2+}, Co^{2+}, and Mn^{2+}. *J. Chem. Phys.* **1961,** *35*, 1483-1490.

(14) Drickamer, H. G. The effect of high pressure on the electronic structure of solids. *Ber. Bunsenges. Phys. Chem.* **1966,** *70*, 952-957.

(15) Reber, C.; Grey, J. K.; Lanthier, E.; Frantzen, K. A. Pressure-induced change of d-d luminescence energies, vibronic structure and band intensities in transition metal complexes. *Comments Inorg. Chem.* **2005,** *26*, 233-254.

(16) Trueba, A.; Garcia-Fernandez, P.; Garcia-Lastra, J. M.; Aramburu, J. A.; Barriuso, M. T.; Moreno, M. Spectrochemical series and the dependence of Racah and 10 Dq parameters on the metal-ligand distance: microscopic origin. *J. Phys. Chem. A* **2011,** *115*, 1423-1432.

(17) Poirier, S.; Tailleur, E.; Lynn, H.; Reber, C. Characterization of Pd···H-C interactions in bis-dimethyldithiocarbamate palladium(II) and its deuterated analog by luminescence spectroscopy at variable pressure. *Dalton Trans.* **2016,** *45*, 10883-10886.

(18) Gliemann, G.; Yersin, H. Spectroscopic properties of the quasi one-dimensional tetracyanoplatinate(II) compounds. *Struct. Bonding* **1985,** *62*, 87-153.

(19) Zahner, J. C.; Drickamer, H. G. Pressure Effects in Nickel Dimethylglyoxime and Related Chelates. *J. Chem. Phys.* **1960,** *33*, 1625-1628.
(20) Tkacz, M.; Drickamer, H. G. High pressure study of changes in energy and intensity of excitations in crystalline metal glyoximes. *J. Chem. Phys.* **1986,** *85*, 1184-1189.
(21) Levasseur-Thériault, G.; Reber, C.; Aronica, C.; Luneau, D. Large pressure-induced red shift of the luminescence band originating from nonstacked square-planar $[Pt(SCN)_4]^{2-}$ in a novel trimetallic complex. *Inorg. Chem.* **2006,** *45*, 2379-2381.
(22) Poirier, S.; Czympiel, L.; Bélanger-Desmarais, N.; Mathur, S.; Reber, C. Temperature and pressure variations of d-d luminescence band maxima of bis(pyridylalkenolato)palladium(II) complexes with different ligand substituents: opposite-signed trends. *Dalton Trans.* **2016,** *45*, 6574-6581.
(23) Brookhart, M.; Green, M. L.; Parkin, G. Agostic interactions in transition metal compounds. *Proc. Natl. Acad. Sci. U.S.A.* **2007,** *104*, 6908-6914.
(24) Yao, W.; Eisenstein, O.; Crabtree, R. H. Interactions between C···H and N···H bonds and d^8 square planar metal complexes: hydrogen bonded or agostic? *Inorg. Chim. Acta.* **1997,** *254*, 105-111.
(25) Sassmannshausen, J. Quo vadis, agostic bonding? *Dalton Trans.* **2012,** *41*, 1919-1923.
(26) Singh, S. K.; Drew, M. G. B.; Singh, N. Self assembly of homoleptic Ni(II) dithiocarbamates and dithiocarbimates via Ni···H–C anagostic and C–H···π (chelate) interactions. *Cryst. Eng. Comm.* **2013,** *15*, 10255-10265.
(27) Siddiqui, K. A.; Tiekink, E. R. A supramolecular synthon approach to aid the discovery of architectures sustained by C-H···M hydrogen bonds. *Chem. Commun.* **2013,** *49*, 8501-8503.
(28) Colby, D. A.; Bergman, R. G.; Ellman, J. A. Rhodium-catalyzed C-C bond formation via heteroatom-directed C-H bond activation. *Chem. Rev.* **2010,** *110*, 624-655.
(29) Hall, C.; Perutz, R. N. Transition Metal Alkane Complexes. *Chem. Rev.* **1996,** *96*, 3125-3146.
(30) Lein, M. Characterization of agostic interactions in theory and computation. *Coord. Chem. Rev.* **2009,** *253*, 625-634.
(31) Housecroft, C. E.; Sharpe, A. G. *Inorganic Chemistry*. Second ed.; Pearson Education Limited: England, 2005; p 949.
(32) Shriver, D. F.; Atkins, P. W. *Chimie inorganique*. De Boeck Université: France, 2001; p 763.
(33) Cotton, F. A.; Wilkinson, G.; Gaus, P. L. *Basic Inorganic Chemistry*. Third ed.; John Wiley & Sons, Inc.: Canada, 1995; p 838.
(34) Wölpl, A.; Oelkrug, D. Lumineszenz von $[Co(CN)_6]^{3-}$, $[Rh(CN)_6]^{3-}$, $[Ir(CN)_6]^{3-}$ mit verschiedenen Gegenionen. *Ber. Bunsenges. Phys. Chem.* **1975,** *79*, 394-400.
(35) Yersin, H.; Otto, H.; Zink, J. I.; Gliemann, G. Franck-Condon analysis of transition-metal complexes. *J. Am. Chem. Soc.* **1980,** *102*, 951-955.
(36) Pelletier, Y.; Reber, C. Near-Infrared Electronic Spectroscopy and Emitting-State Properties of K_2PdCl_4 and K_2PdBr_4. *Inorg. Chem.* **1997,** *36*, 721-728.
(37) Genre, C.; Levasseur-Thériault, G.; Reber, C. Emitting-state properties of square-planar dithiocarbamate complexes of palladium(II) and platinum(II) probed by pressure-dependent luminescence spectroscopy. *Can. J. Chem.* **2009,** *87*, 1625-1635.
(38) Poirier, S.; Rahmani, F.; Reber, C. Large d-d luminescence energy variations in square-planar bis(dithiocarbamate) platinum(II) and palladium(II) complexes with near-identical MS_4 motifs: a variable-pressure study. *Dalton Trans.* **2017,** *46*, 5279-5287.
(39) Poirier, S.; Roberts, R. J.; Le, D.; Leznoff, D. B.; Reber, C. Interpreting Effects of Structure Variations Induced by Temperature and Pressure on Luminescence Spectra of Platinum(II) Bis(dithiocarbamate) Compounds. *Inorg. Chem.* **2015,** *54*, 3728-3735.
(40) Poirier, S.; Guionneau, P.; Luneau, D.; Reber, C. Why do the luminescence maxima of isostructural palladium(II) and platinum(II) complexes shift in opposite directions? *Can. J. Chem.* **2014,** *92*, 958-965.
(41) Grey, J. K.; Marguerit, M.; Butler, I. S.; Reber, C. Pressure-dependent Raman spectroscopy of metal-oxo multiple bonds in rhenium(V) and osmium(VI) complexes. *Chem. Phys. Lett.* **2002,** *366*, 361-367.

(42) Suffren, Y.; Rollet, F.-G.; Reber, C. Raman Spectroscopy of Transition Metal Complexes: Molecular Vibrational Frequencies, Phase Transitions, Isomers, and Electronic Structure. *Comments Inorg. Chem.* **2011,** *32*, 246-276.
(43) Woinska, M.; Grabowsky, S.; Dominiak, P. M.; Wozniak, K.; Jayatilaka, D. Hydrogen atoms can be located accurately and precisely by x-ray crystallography. *Sci. Adv.* **2016,** *2*, e1600192.
(44) Howard, J. A.; Probert, M. R. Cutting-edge techniques used for the structural investigation of single crystals. *Science* **2014,** *343*, 1098-1102.
(45) Shannon, R. D. Revised effective ionic radii and systematic studies of interatomic distances in halides and chalcogenides. *Acta Cryst.* **1976,** *32*, 751-767.
(46) Guionneau, P.; Collet, E. In *Spin-Crossover Materials: Properties and Applications*; HALCROW, M. A., Ed.; John Wiley & Sons Ltd: Oxford, UK, 2013; pp 507-526.
(47) Casati, N.; Genoni, A.; Meyer, B.; Krawczuk, A.; Macchi, P. Exploring charge density analysis in crystals at high pressure: data collection, data analysis and advanced modelling. *Acta Crystallogr. B* **2017,** *73*, 584-597.
(48) Grey, J. K.; Butler, I. S.; Reber, C. Pressure-induced enhancements of luminescence intensities and lifetimes correlated with emitting-state distortions for thiocyanate and selenocyanate complexes of platinum(II) and palladium(II). *Inorg. Chem.* **2003,** *42*, 6503-6518.
(49) Van Houten, J.; Watts, R. J. Effect of ligand and solvent deuteration on the excited state properties of the tris(2,2'-bipyridyl)ruthenium(II) ion in aqueous solution. Evidence for electron transfer to solvent. *J. Am. Chem. Soc.* **1975,** *97*, 3843-3844.
(50) Li, R.; Lim, E. C. Quantitative Study of Luminescence in Aromatic and Heteroaromatic Molecules. *J. Chem. Phys.* **1972,** *57*, 605-612.
(51) Hirota, N.; Hutchison, C. A. Effect of Deuteration of Durene on the Lifetime of the Phosphorescent Triplet State of Naphthalene in a Durene Host Crystal. *J. Chem. Phys.* **1967,** *46*, 1561-1564.
(52) Sørensen, M. A.; Weihe, H.; Vinum, M. G.; Mortensen, J. S.; Doerrer, L. H.; Bendix, J. Imposing high-symmetry and tuneable geometry on lanthanide centres with chelating Pt and Pd metalloligands. *Chem. Sci.* **2017,** *8*, 3566-3575.
(53) Dolomanov, O. V.; Bourhis, L. J.; Gildea, R. J.; Howard, J. A. K.; Puschmann, H. OLEX2: a complete structure solution, refinement and analysis program. *J. Appl. Crystallogr.* **2009,** *42*, 339-341.
(54) Sheldrick, G. M. Crystal structure refinement with SHELXL. *Acta Crystallogr. C* **2015,** *71*, 3-8.
(55) Sheldrick, G. M. A short history of SHELX. *Acta. Crystallogr. A* **2008,** *64*, 112-122.
(56) Probert, M.; Coome, J.; Goeta, A.; Howard, J. Silver the new gold standard for high-pressure single crystal X-ray diffraction. *Acta Crystallogr., Sect. A: Found. Crystallogr* **2011,** *67*, C528.
(57) Sheldrick, G. M. Bruker AXS Inc., Madison, WI *Bruker Apex II* **2004**.
(58) Parsons, S. ECLIPSE, The University of Edinburgh, Edinburgh, UK. **2009**.
(59) SAINT. Bruker AXS Inc., Madison, WI. **2007**.
(60) SADABS. Bruker AXS Inc., Madison, WI. **2001**.

Tables

Table 1. Results of linear fits for luminescence maxima E_{max} at ambient pressure and pressure induced shift $\Delta E_{max}/\Delta P$ for $[M\{(CH_3)_2DTC\}_2]$ and $[M\{(CD_3)_2DTC\}_2]$ complexes.

Metal M	**Substituent on ligand**	**Fitted $E_{max, P=0}$ (cm^{-1})**	**Fitted $\Delta E_{max}/\Delta P$ (cm^{-1}/kbar)**		
			0-20 kbar	**20-40 kbar**	**> 45 kbar**
Ni(II)	CH_3	13531 ± 64	+26 ± 5	-15 ± 6	
	CD_3	13611 ± 104	+20 ± 5	N/A	
Pd(II)	CH_3	13003 ± 47	+32 ± 3	+11 ± 3	-31 ± 8
	CD_3	12345 ± 89	+63 ± 8	+12 ± 5	N/A
Pt(II)	CH_3	13472± 73	+44 ± 5		-37 ± 8
	CD_3	N/A	N/A		

Table 2. Selected bond lengths and angles for [Ni{$(CH_3)_2DTC$}$_2$], [Pd{$(CH_3)_2DTC$}$_2$] and [Pt{$(CH_3)_2DTC$}$_2$] and their deuterated analogs, [Ni{$(CD_3)_2DTC$}$_2$], [Pd{$(CD_3)_2DTC$}$_2$] and [Pt{$(CD_3)_2DTC$}$_2$] at room temperature, with measured H and D positions.

	[M{$(CH_3)_2DTC$}$_2$]			[M{$(CD_3)_2DTC$}$_2$]		
Bonds (Å)	**Ni(II)**	**Pd(II)**	**Pt(II)**	**Ni(II)**	**Pd(II)**	**Pt(II)**
M-S(1)	2.212(1)	2.3334(4)	2.3281(7)	2.2109(8)	2.3324(9)	2.329(2)
M-S(2)	2.1924(8)	2.3136(3)	2.3118(6)	2.1927(7)	2.3148(6)	2.313(2)
C(1)-S(1)	1.718(8)	1.722(1)	1.722(2)	1.716(3)	1.722(4)	1.724(8)
C(1)-S(2)	1.718(3)	1.724(1)	1.733(2)	1.716(3)	1.734(3)	1.740(7)
C(1)-N(1)	1.325(4)	1.313(2)	1.307(3)	1.331(3)	1.300(4)	1.299(9)
C(2)-N(1)	1.447(6)	1.459(3)	1.462(4)	1.439(6)	1.457(7)	1.45(1)
C(3)-N(1)	1.449(5)	1.460(2)	1.463(4)	1.448(5)	1.459(6)	1.47(1)
Angles (°)						
S(1)-M-S(2)	79.45(4)	75.54(1)	75.10(2)	79.46(3)	75.45(3)	75.10(7)
S(1)-C(1)-S(2)	110.0(2)	111.40(8)	109.9(1)	110.2(2)	110.7(2)	109.5(4)
N(1)-C(1)-S(1)	124.7(3)	123.8(1)	124.8(2)	124.6(2)	124.5(3)	125.2(6)
N(1)-C(1)-S(2)	125.3(3)	124.8(1)	125.3(2)	125.2(2)	124.8(3)	125.2(6)
C(2)-N(1)-C(3)	116.6(3)	116.0(1)	116.0(2)	116.8(3)	115.8(4)	115.6(8)

Table 3. Selected intermolecular distances for [Ni{$(CH_3)_2DTC$}$_2$], [Pd{$(CH_3)_2DTC$}$_2$] and [Pt{$(CH_3)_2DTC$}$_2$] and their deuterated analogs, [Ni{$(CD_3)_2DTC$}$_2$], [Pd{$(CD_3)_2DTC$}$_2$] and [Pt{$(CD_3)_2DTC$}$_2$] at room temperature, with measured H and D positions.

Intermolecular[a] distance (Å) or angle (°)	**[M{$(CH_3)_2DTC$}$_2$]**			**[M{$(CD_3)_2DTC$}$_2$]**		
	Ni(II)	**Pd(II)**	**Pt(II)**	**Ni(II)**	**Pd(II)**	**Pt(II)**
M···H or M···D	2.89(7)	3.01(3)	2.99(6)	2.96(6)	3.00(8)	3.1(3)
M···C	3.722(6)	3.811(2)	3.886(4)	3.733(5)	3.818(6)	3.89(1)
M···H-C or M···D-C	149(5)	154(2)	156(4)	151(4)	147(5)	148(23)
S(1)-M···H or S(1)-M···D	82(1)	77.0(5)	74(1)	80(1)	77(1)	74(5)
S(2)-M···H or S(2)-M···D	89(1)	85.9(5)	84(1)	88(1)	88(1)	85(5)
S(1)'-M···H or S(1)'-M···D	91(1)	94.1(5)	96(1)	92(1)	92(1)	95(5)
S(2)'-M···H or S(2)'-M···D	98(1)	103.0(5)	106(1)	100(1)	103(1)	106(5)

[a]Values from the shortest intermolecular distance.

Table 4. Selected bond lengths, angles and intermolecular distances for [Pt{$(CH_3)_2$DTC}$_2$] at variable pressure and room temperature.

	Pressure		
Bonds (Å)	Amb.	5 kbar	10 kbar
Pt-S(3)	2.32(1)	2.314(5)	2.31(1)
Pt-S(2)	2.326(7)	2.333(7)	2.33(1)
C(1)-S(3)	1.70(3)	1.70(2)	1.68(7)
C(1)-S(2)	1.71(4)	1.71(3)	1.69(5)
C(1)-N(1)	1.40(3)	1.36(2)	1.30(5)
C(5)-N(1)	1.46(6)	1.46(3)	1.54(9)
C(4)-N(1)	1.41(5)	1.48(4)	1.56(7)
Angles (°)			
S(2)-Pt-S(3)	75.4(3)	75.1(2)	75.2(5)
S(2)-C(1)-S(3)	113(2)	112(2)	114(4)
N(1)-C(1)-S(2)	121(3)	125(2)	124(5)
N(1)-C(1)-S(3)	125(3)	122(2)	122(5)
C(4)-N(1)-C(5)	118(3)	116(2)	110(5)
Intermolecular distances (Å)			
Pt···H(A)	2.99	2.95	2.98
Pt···H(D)	4.14	3.63	3.47
Pt···C(4)	3.89(6)	3.84(4)	3.82(9)
Pt···C(5)	4.39(4)	4.34(3)	4.18(6)
S(2)···S(3)	4.48(2)	4.41(1)	4.33(2)
S(2)···H(E)[a]	3.10(1)	2.742(6)	2.79(1)
S(3)···S(3)[a]	3.84(1)	3.752(9)	3.64(2)
S(3)···S(2)[a]	3.74(1)	3.694(8)	3.63(2)
Intermolecular angles (°)			
S(3)-Pt-H(A)	74.5(3)	75.3(2)	74.6(4)
S(2)-Pt-H(A)	83.4(2)	84.7(2)	87.2(4)
S(2)'-Pt-H(A)	96.6(2)	95.3(2)	92.8(4)
S(3)'-Pt-H(A)	105.5(3)	104.7(2)	105.4(4)
S(3)-Pt-C(4)	72.2(7)	72.0(5)	72(1)
S(2)-Pt-C(4)	78.2(7)	78.6(5)	80(1)
S(2)'-Pt-C(4)	101.8(7)	101.4(5)	100(1)
S(3)'-Pt-C(4)	107.8(7)	108.0(5)	108(1)

[a] Intermolecular distances for two complexes in the same plane as the ML_4 motif.

Figures

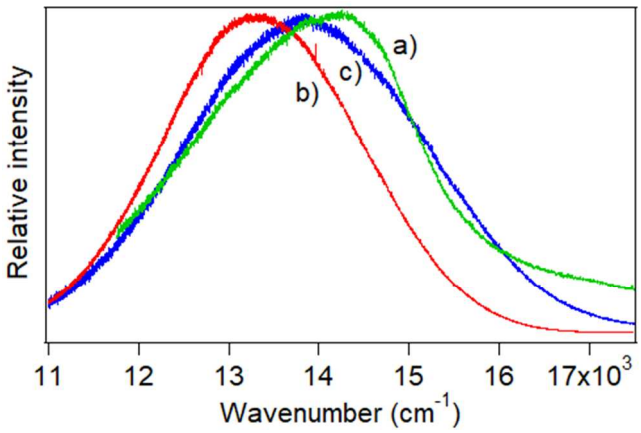

Figure 1. Luminescence spectra at 80 K and ambient pressure for [Ni{$(CH_3)_2$DTC}$_2$] (a, green), [Pd{$(CH_3)_2$DTC}$_2$] (b, red) and [Pt{$(CH_3)_2$DTC}$_2$] (c, blue).

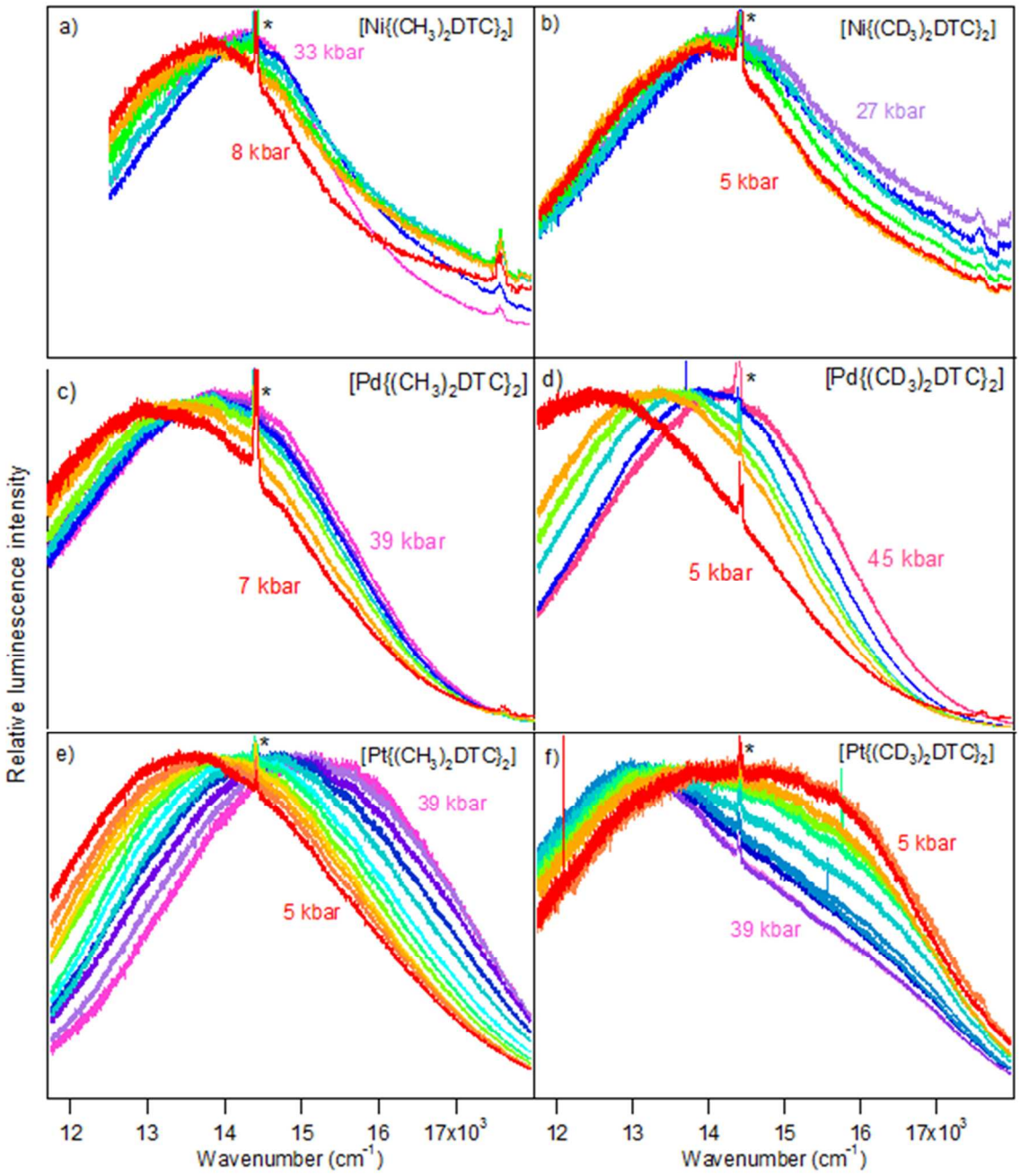

Figure 2. Luminescence spectra at variable pressure for [Ni{$(CH_3)_2DTC\}_2$] (a), [Ni{$(CD_3)_2DTC\}_2$] (b), [Pd{$(CH_3)_2DTC\}_2$] (c), [Pd{$(CD_3)_2DTC\}_2$] (d), [Pt{$(CH_3)_2DTC\}_2$] (e) and [Pt{$(CD_3)_2DTC\}_2$] (f). Asterisks mark the ruby R-line used for pressure calibration.

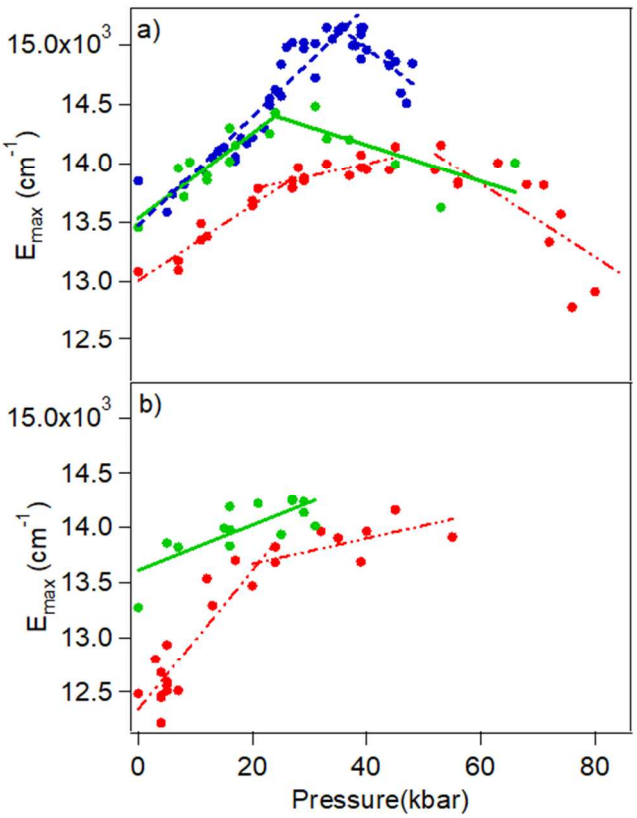

Figure 3. Variable-pressure luminescence maxima E_{max} of $[M\{(CH_3)_2DTC\}_2]$ (a) and $[M\{(CD_3)_2DTC\}_2]$ (b) complexes with pressure. Maxima for nickel(II) complexes are presented in green (solid lines for trends), for palladium(II) complexes in red (dotted lines) and platinum(II) in blue (dashed lines).

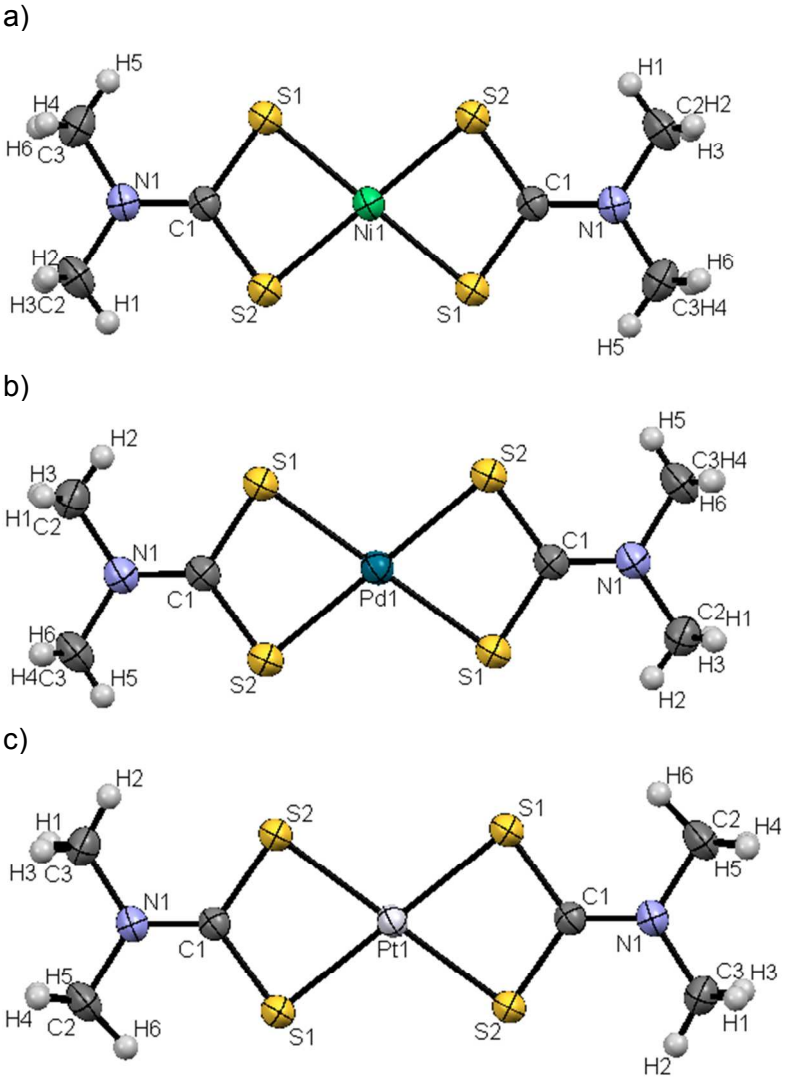

Figure 4. Perspective views of high resolution structures for [Ni{$(CH_3)_2$DTC}$_2$] (a), [Pd{$(CH_3)_2$DTC}$_2$] (b) and [Pt{$(CH_3)_2$DTC}$_2$] (c). Ellipsoids are shown at 50% probability.

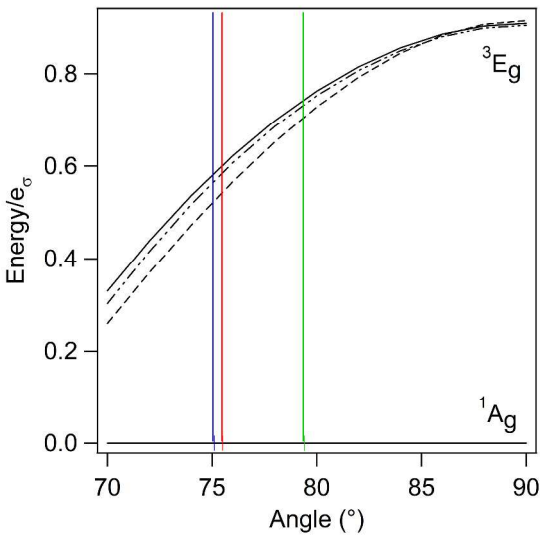

Figure 5. Energy difference between the lowest-energy excited state (^3E_g) and the ground state (^1A_g) as a function of the S-M-S angle (°). The solid line denotes for σ donor ligands ($e_\pi = 0$), the dashed line is for π donor ligands ($e_\sigma / e_\pi = 4.4$) and the dotted-dashed line is for π acceptor ligands ($e_\sigma / e_\pi = -4.4$). Values of 600 cm^{-1} and 2400 cm^{-1} were used for the Racah B and C parameters. The vertical lines indicate experimental S-M-S angles for platinum(II) (blue), palladium(II) (red) and for nickel(II) (green).

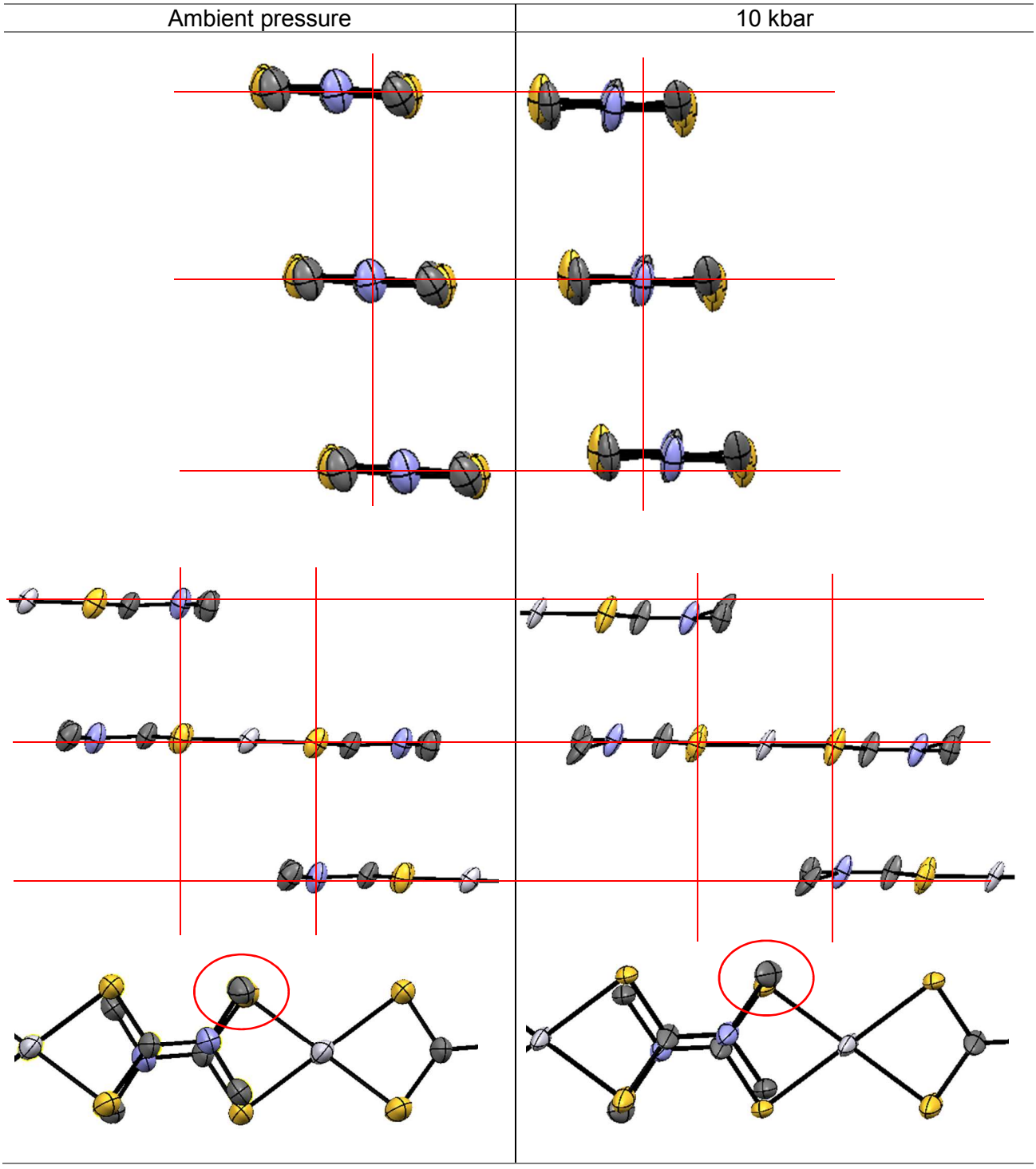

Figure 6. Three different views of three molecules of $[Pt\{(CH_3)_2DTC\}_2]$ at ambient pressure (left) and 10 kbar (right). Horizontal and vertical lines (red) are drawn as guide to the eye. Hydrogen atoms are omitted for clarity.